CONF-8706258--4

CONF-8706258--4

DE88 010085

Solidus and Liquidus Temperatures in the Uranium–Plutonium–Zirconium System*

L. Leibowitz, E. Veleckis, R. A. Blomquist

Argonne National Laboratory, Chemical Technology Division, 9700 S. Cass Avenue, Argonne IL 60439 USA

and A. D. Pelton

Ecole Polytechnique, Université de Montréal, Montréal, Québec, Canada

Abstract: Renewed interest in metallic fuel for nuclear reactors has prompted study of the solidus and liquidus for the uranium–plutonium–zirconium system. These temperatures are of importance in assessing the possibility of fuel melting during abnormal reactor conditions. Data obtained in previous work in this area were found to be inadequate for the needs of the current reactor development effort. A dual effort was undertaken to provide the needed data. These were (1) thermodynamic phase diagram analysis and calculation of the ternary solidus and liquidus surfaces and (2) experimental determination of solidus and liquidus temperatures for selected alloys. The methods used and results obtained are described.

1. Introduction

Recently increased interest in metallic fuels for liquid–metal fast breeder reactors has prompted a reassessment of the available thermodynamic and transport property data. Of particular importance are the solidus and liquidus surfaces for the uranium–plutonium–zirconium system. These temperatures are important in assessing the possibility of fuel melting during off–normal conditions. Some work has appeared in the literature on this subject in the past (1), but the previously available data were inadequate in scope and reliability for present purposes. To supply the needed data, we are employing a dual approach that involves thermodynamic calculation and experimental determination of solidus and liquidus temperatures for selected alloys. It is intended that, as measured values become available, the thermodynamic calculations will be improved to reflect those new data. In the following paper, we report on the methods used and results obtained for this ongoing work.

2. Calculational

2.1 Introduction

The techniques of thermodynamic phase diagram analysis have been well documented

*This work supported by the U. S. Department of Energy

(2-5). When applied to the computation of an unknown ternary phase diagram, these techniques involve the critical evaluation and analysis of all relevant phase diagram and thermodynamic data for the three binary sub-systems with a view of obtaining mathematical expressions for the thermodynamic properties of all binary phases as functions of composition and temperature. Following this, interpolation techniques based upon solution models are used to estimate the thermodynamic properties of the ternary phases from the properties of the binary phases. The ternary phase diagram is then calculated from the estimated ternary Gibbs energy surfaces. All calculations are performed with programs of the F*A*C*T (Facility for the Analysis of Chemical Thermodynamics) computer system based in Montreal (2). For the Pu-U-Zr system, a liquid solution and a body-centered-cubic (bcc) solid solution exist at all compositions within the ternary system. Liquidus and solidus curves have been reported for all three binary sub-systems, but virtually no data on the ternary liquidus or solidus are available.

In solutions in which deviations from ideal behavior are not large, polynomial expansions of the excess Gibbs energy (G^E) in terms of the molar fractions are commonly used. In a binary system with components A and B, the excess Gibbs energy is given by:

$$G^E = X_A X_B (a_o + a_1 X_B + a_2 X_B^2 + \cdots) \qquad [1]$$

where X_A and X_B are the molar fractions, and $a_o, a_1, a_2, \cdots$ are empirical coefficients to be determined. It should be noted that

$$G^E \equiv RT(X_A \ln\gamma_A + X_B \ln\gamma_B) \qquad [2]$$

where γ_A and γ_B are the activity coefficients. In general, G^E varies with T, but for the Pu-U-Zr system the available data are insufficient to determine the temperature dependence. Thus it is assumed that G^E (and hence all coefficients $a_o, a_1, a_2, \cdots$) is independent of temperature. This is equivalent to assuming zero excess entropy.

If all coefficients $a_o, a_1, a_2 \cdots$ are zero, then the solution is "ideal". If only a_o is nonzero, then the solution is "regular." If a_o and a_1 are nonzero, then the solution is "sub-regular."

In the present case, no more than three coefficients (a_o, a_1, and a_2) were ever required in any binary solution.

2.2 Melting Points, Enthalpies, and Gibbs Energies of Melting

The Gibbs energies of melting of all three components of the alloy are required in the present analysis. In the equations which follow, the Gibbs energy of melting ($\Delta G^{\circ}_{fusion}$) is in cal/mol and the temperature (T) is in K.

Data for Pu are reviewed by Oetting et al. (6). A melting point of 640±2°C and an enthalpy of melting of 680±25 cal/mol are given. Heat capacities of the solid and liquid are also known with reasonable accuracy. The resultant expression for the Gibbs energy of melting is

$$\Delta G^{\circ}_{fusion(Pu)} = -786 + 11.768\ T - 1.600\ T \ln T \qquad [3]$$

For Zr, data are taken from the JANAF tables (7). The melting point is 1852 ±5°C and the enthalpy of fusion is 5000 ±7% cal/mol. Solid and liquid heat capacities are also given in the JANAF tables (7). The resultant Gibbs energy of melting expression is

$$\Delta G^{\circ}_{fusion(Zr)} = 2308 + 16.474\ T + 5.550\ X\ 10^{-4}\ T^2 - 2.446\ T \ln T \qquad [4]$$

The data for U were reviewed by Oetting et al. (6). The melting point is 1132±3°C. Two determinations of the enthalpy of fusion of uranium (8,9) were discussed (6) and the more recent calorimetric value (8), 2185 cal/mol, was selected. There is, however, a third experimental value (10) of 2.9 cal/mol, as well as estimates of 3.25 cal/mol (11) from vapor pressure data and 2.5 cal/mol (12) from an assessment of uranium alloy phase diagrams. As is shown in a later section of this report on the Pu-U binary system, the value of 2185 cal/mol gives poor agreement with the measured phase diagram. The Savage and Seibel (10) value of 2900 cal/mol is preferred. In view of the uncertainty in the enthalpy of fusion of U, we simply assumed that this value is independent of temperature, such that

$$\Delta G^{\circ}_{fusion(U)} = 2900 - 2.0641\ T \qquad [5]$$

2.3 Analysis of Binary Systems

Examination of the three binary systems was performed to provide excess Gibbs energy equations which were required for ternary system calculations. In addition, estimates were made of the uncertainties in binary solidus and liquidus temperatures based on the available data and thermodynamic consistency. As is shown below, the estimated uncertainties differed considerably among the three binary sub-systems.

The Pu-Zr System

The liquidus and solidus for Pu-Zr have been measured up to about 50 mol % Zr by Marples (13) and Bochvar et al. (14). These two studies disagree by as much as 50°C in the liquidus and 100°C in the solidus. Study by Taylor (18) for Zr concentrations up to 10 mol % gave a solidus close to that of Bochvar et al. (14) but a liquidus 40°C higher than either Marples (13) or Bochvar et al. (14) at 10% Zr. In a fourth study (19), which can probably be discounted, liquidus temperatures 200°C higher than those of all other authors were reported at Zr concentrations near 15 mol %. The work of Marples (13) appears to be the most extensive, and so more weight was given to the results of this study in the analysis. This was also the opinion of Shunk (17) in his compilation.

Under the assumption of ideal liquid behavior and regular solution behavior for the solid with

$$G^{E}_{(sol)} = 1600\ X_{Pu}X_{Zr}\ \text{cal/mol} \qquad [6]$$

the diagram shown in Fig. 1 was calculated. This figure shows that the calculated diagram is a compromise between the various reported diagrams, but that more weight is given to the diagram of Marples (13). The existence of small positive deviations in the solid phase (15,16) is supported by the shape of the two-phase ϵ/δ region, which passes through a maximum at 640°C. For this binary system, error limits are estimated as ±50°C for the liquidus and ±100°C for the solidus.

The Pu-U System

The liquidus and solidus for Pu–U have been measured by Ellinger et al. (20) and by Mound Laboratory (21). The liquidus curves of these two studies agree to within better than 15°C, but the solidus curves diverge by up to 40°C. Ellinger et al. (20) state that they experienced difficulty in obtaining reproducible solidus measurements. They reported the minimum to be at 610°C and 12 mol % U on the basis of their solidus points. However, their liquidus measurements place the minimum closer to 620°C, which is the minimum temperature reported by Mound Laboratory (21). Another author (22) reports a minimum at 624°C and 9 mol % U.

Activity measurements in the liquid phase are reviewed by Chiotti et al. (23). Although the results suggest negative deviations in the liquid, they are so imprecise and their interpretation involves so many assumptions that they should be viewed cautiously. It is simpler, and also more concordant with experience in other alloy systems, to assume that the solidus/liquidus minimum is the result of small positive deviations in the solid. This contention is supported by the shape of the two-phase ϵ/η, region which passes through a maximum.

The liquidus in this system seems to be relatively accurately known. Under the assumption that the liquidus is correct, it can be shown (24) that the solidus as well as $G^{E}_{(sol)}$ can be exactly calculated if the enthalpies of fusion of the components as well as $G^{E}_{(liq)}$ are known. We performed such calculations assuming ideal liquid behavior, using eq. [3] for the enthalpy of fusion of Pu,and taking the enthalpy of fusion of U to be 2185 cal/mol (6). The resulting $G^{E}_{(sol)}$ was small, sub-regular, and well behaved, but the calculated solidus was up to 25°C above that reported by Mound Laboratory (21) and 65°C above that reported by Ellinger et al. (20). Assuming a negative $G^{E}_{(liq)}$ as suggested by Chiotti et al. (23) makes things worse. Fair agreement can be obtained if quite large positive excess Gibbs energies in both solid and liquid phases, which nearly compensate each other, are assumed. However, this seems improbable. It is more likely that either (i) the reported solidus curves are in

error, or (ii) the enthalpy of fusion of U is higher than 2185 cal/mol. The latter option seems more attractive in view of the wide range of values of the enthalpy of fusion of U which have been reported. With the enthalpy of fusion of U set at 2900 cal/mol, the value of Savage and Seibel (10), the solidus shown in Fig. 2 was calculated. $G^E_{(sol)}$ is given by a three-term expression:

$$G^E_{(sol)} = X_{Pu}X_U\ (1207 + 572\ X_U - 1080\ X_U^2)\ \text{cal/mol} \qquad [7]$$

The calculated liquidus is everywhere within 10°C of that reported by Ellinger at al. (20). The calculated minimum is at 672°C and X_U=0.10.

Although this analysis seems to be a reasonable solution to the problem posed by the inconsistency of the various data sets, it is disquieting that $G^E_{(sol)}$ is now larger and requires a three-term expression and that the most recent calorimetric measurements of the enthalpy of fusion of U should be so much in error. Hence, one cannot eliminate the possibility that the real solidus is higher than the calculated value by up to 35°C. For this reason, error limits are set at ±15°C for the liquidus and ±40°C for the solidus.

Zr-U System

The solidus and liquidus for Zr-U have been measured in only one study (25). Another study (19) gives no data but reports that "solidus and liquidus temperatures are in agreement" with those of Summers-Smith (25) up to 50% Zr. A "lens-shaped" two-phase region in the phase diagram of Summers-Smith (25) is indicative of close-to-ideal behavior in both solid and liquid phases. However, the existence of a solid-solid miscibility gap at lower temperatures indicates quite strong positive deviations in the solid phase. Furthermore, the fact that the consolute composition of the gap is displaced toward higher uranium concentrations indicates that the positive deviations are quite asymmetric (nonregular). These positive deviations in the solid should then be expected to give rise to a minimum in the liquidus/solidus. That there is no such minimum can only be explained if the liquid phase also exhibits nonregular and nearly compensating positive deviations. Such behavior is unusual, and these observations thus add to the uncertainty surrounding the liquidus/solidus of this

system. Activity measurements in the solid solution as reviewed by Chiotti et al. (23) are so imprecise as to be of little value in the analysis.

More recent measurements (26) of the solid-solid miscibility gap place the consolute point at 772°C and X_U=0.70, with boundaries at the eutectoid temperature of 693°C at X_U=0.576 and X_U=0.89. These results are quite different from those of Summers–Smith (25) but are preferred by Shunk (17) in his compilation on the basis of better experimental technique. The following equation was then calculated in order to reproduce the eutectoid compositions:

$$G^E_{(sol)} = X_{Zr}X_U\ (-688 + 5123\ X_U)\ \text{cal/mol} \qquad [8]$$

Under the assumption of sub-regular behavior for the liquid, the following equation was computed in order to give a reasonable reproduction of the measured liquidus and solidus points:

$$G^E_{(liq)} = X_{Zr}X_U\ (0 + 3800\ X_U)\ \text{cal/mol} \qquad [9]$$

The calculated diagram is shown in Fig. 3. The S-shape of the solidus at high U concentrations is a direct result of the positive deviations in the solid. The narrowness of the two–phase (liquid + solid) region at high Zr concentrations is a consequence of the enthalpy of fusion of Zr and must be reasonably correct. This system is not well characterized. Error limits should probably be set at ±75°C for the liquidus and ±75°C for the solidus.

2.4 Calculation of the Ternary Phase Diagram

Excess Gibbs energies in the ternary liquid and solid phases were calculated from the values for the three binary systems by means of the "Kohler interpolation equations" (27)

$$G^E = (1 - X_{Pu})^2\ G^E_{U/Zr} + (1 - X_U)^2\ G^E_{Zr/Pu} + (1 - X_{Zr})^2 G^E_{U/Pu} \qquad [10]$$

in which G^E at a ternary composition point is calculated from the values $G^E_{U/Zr}$, $G^E_{Zr/Pu}$, and $G^E_{U/Pu}$ in the three binary systems at the same values of the ratios X_U/X_{Zr}, X_{Zr}/X_{Pu}, and

X_U/X_{Pu} as at the ternary point. This equation has been used extensively for ternary alloy systems (3,4).

Representative calculated ternary solidus and liquidus curves are shown in Figs. 4. Error limits for ternary compositions lying near a binary edge of the ternary composition triangle are approximately the same as the error limits at adjacent compositions in that binary, as given in the preceding section. For compositions near the center of the ternary composition triangle, an additional uncertainty due to the approximate nature of the Kohler interpolation technique must be included. Near the median of the composition triangle ($X_{Pu} = X_U = X_{Zr}=1/3$), error limits are estimated as $\pm 75^{\circ}C$ for the liquidus and $\pm 125^{\circ}C$ for the solidus.

Ternary isotherms in the Pu corner of the diagram are reported by the Mound Laboratory (19). However, that study gives liquidus temperatures in the Pu-Zr binary which are $200^{\circ}C$ higher near 15 mol % Zr than those reported by any other author. Hence, these results should be discounted. Nevertheless, the general shape of the reported isotherms is the same as that of the calculated isotherms.

We calculated activity coefficients in both ternary phases by differentiation of the Kohler equation. The calculated activity coefficients were referred to the pure bcc solids as standard states for the solid solution and to the pure liquids for the liquid solution.

In the following expressions for activity coefficients, the components are numbered Pu=1, U=2, and Zr=3 with mole fractions X_1, X_2, X_3. In addition the temperature (T) is in K, ln represents natural logarithms, and R=1.987.

Liquid Solution

$$RT \ln \gamma_1 = -3800 X_2^2 X_3/(1 - X_1) \quad [11]$$

$$RT \ln \gamma_2 = 3800 X_2 X_3 \, (X_1 X_2 + 2X_3)/(1 - X_1)^2 \quad [12]$$

$$RT \ln \gamma_3 = 3800 X_2^2 \, (X_2 - X_3 + X_1 X_3)/(1 - X_1)^2 \quad [13]$$

Solid Solutions

The following general equation may be applied:

$$RT \ln \gamma_k = -(1 - X_k)^2 f_{ij} + (1 - X_i)(f_{k(kj)} + X_i f_{kj}) + (1 - X_j)(f_{k(ki)} + X_j f_{ki}) \qquad [14]$$

$$\begin{aligned} f_{13} &= 1600(1 - t_{13})t_{13} \\ f_{1(13)} &= 1600t_{13}^2 \qquad \text{where } t_{13} = X_3/(X_1 + X_3) \\ f_{3(13)} &= 1600(1 - t_{13})^2 \end{aligned} \qquad [15]$$

$$\begin{aligned} f_{23} &= (1 - t_{23})t_{23}(-688 + 5123t_{23}) \\ f_{2(23)} &= (1 - t_{23})^2(-688 + 10246t_{23}) \qquad \text{where } t_{23} = X_2/(X_2 + X_3) \\ f_{3(23)} &= -5811t_{23}^2 + 10246t_{23}^3 \end{aligned} \qquad [16]$$

$$\begin{aligned} f_{12} &= (1 - t_{12})t_{12}(1207 + 572t_{12} - 1080t_{12}^2) \\ f_{1(12)} &= 635t_{12}^2 + 3304t_{12}^3 - 3240t_{12}^4 \qquad \text{where } t_{12} = X_2/(X_1 + X_2) \\ f_{2(12)} &= (1 - t_{12})^2\,(1207 + 1144t_{12} - 3240t_{12}^2) \end{aligned} \qquad [17]$$

By setting one of the mole fractions equal to zero in eqs. [11-17], activity coefficients in any of the three binary sub-systems can also be calculated. In view of the many approximations which have been made, computed values of $\ln\gamma$ should be considered accurate to within a factor of two.

3. Experimental

3.1 Methods

Solidus and liquidus temperatures were measured using differential thermal analysis (DTA) methods. For this work, a Netzsch Inc. Model STA 409 instrument was installed in a helium–atmosphere glove box suitable for work with plutonium–containing materials. The melting points of high purity aluminum and gold were measured periodically to ensure

that accurate temperatures were being obtained. Melting points withir ±1–2 K of literature values were regularly obtained. Solidus and liquidus temperatures were measured on U–Pu–Zr alloys at heating and cooling rates ranging from 1 to 20 K/min. At low rates, detection of the solidus and liquidus was very difficult. At high rates, shifts in the indicated temperatures were found. Generally, rates between 5 and 10 K/min were employed for the data reported. Crucibles fabricated of beryllia (National Beryllia Corp.) and yttria (prepared by R. Poeppel, Argonne National Laboratory) were heated at 1500°C for several hours and tested for compatibility with U–Pu–Zr alloys. Samples of ternary alloys melted in the beryllia and yttria crucibles were examined by SEM/EDS (all SEM examinations were performed by R. V. Strain, Argonne National Laboratory). The samples heated in yttria (U-19 wt% Pu–10 wt% Zr and U–20 wt% Pu–2 wt% Zr) showed no significant composition gradients within the matrix of the sample and no evidence of interaction with the crucible. The sample melted in beryllia (U–19 wt% Pu–10 wt% Zr), in contrast, showed clear evidence of reaction with the crucible and reduced zirconium concentration in the alloy matrix. It was also found that the zirconium concentration was lower near the edges and bottom than at the center and top. Low solidus and liquidus temperatures for the alloy were found in the beryllia crucible and evidently result from a reduced zirconium concentration caused by reaction with the beryllia crucible. All subsequent measurements were performed in yttria DTA crucibles. Alloys for this study were parts of batches prepared by injection casting for irradiation exposure in the EBR–II reactor.

In a typical DTA measurement, a cylindrical sample of alloy about 5 mm high and 5 mm in diameter was cleaned and placed in the DTA crucible and mounted on the sample thermocouple in the DTA system. An identical crucible containing platinum was mounted on the reference thermocouple. The furnace was lowered into position and the system was pumped and flushed several times with high–purity helium. The system was finally filled with high–purity helium to a pressure slightly above ambient. The desired number of heating and cooling cycles were then performed and data were recorded. The STA 409 instrument

includes a thermogravimetry capability, and weight changes were frequently followed during the DTA runs. No significant weight changes were ever detected.

3.2 Results

Sample Morphology

The as–cast fuel of overall composition U–19 wt% Pu–10 wt% Zr, shown in Fig. 5, contains small, nearly spherical particles about 5–10 microns in diameter referred to as the "globular phase." The only metal detectable in this phase using SEM/EDS methods is zirconium, which is presumed to be α–Zr stabilized by oxygen or nitrogen. Following measurements of solidus and liquidus temperatures, this globular Zr phase was found almost entirely at the top of the sample, evidently having floated to the top while the alloy was molten. The remainder of the alloy was totally free of this material with the exception of a small amount at the very bottom. This material may be mechanically removed from the frozen ingot and a very clean alloy sample obtained. The zirconium concentration of the globule–free ternary–alloy phase was quite uniform and was about 7 wt% .

The Zr–rich globular phase appeared in a layer at the surface and in globules about 50–100 microns in diameter (Fig. 6). This size was about 10 times larger than was seen in the as–cast fuel. In addition, very small U–Pu–containing inclusions (Fig. 7), about 1 micron in diameter or less, were seen uniformly distributed within the large Zr–rich globules. The large globules may have resulted from simple agglomeration of the smaller ones with some of the matrix alloy trapped within it. The Zr–rich phase, however, appears to have formed from a liquid and there may exist a previously unknown multi–component Zr–rich phase, which is liquid at about 1500°C and is immiscible in the U–Pu–Zr matrix alloy. No liquid phases exist in either the Zr–O or Zr–N systems below the melting point of pure Zr. Investigation of this phenomenon is continuing.

Solidus/Liquidus Temperatures

Results of measurement of solidus and liquidus temperatures on three alloys are presented in Table 1. The compositions listed in Table 1 were determined by SEM/EDS follow-

ing th melting measurements. The uncertainties given for the measurements are standard deviations (σ) calculated from measurements performed at heating/cooling rates of 5–10 K/min. Calculated values for the solidus and liquidus are also given in Table 1.

Table 1. Solidus and Liquidus Temperatures of U–Pu–Zr Alloys

Alloy (at.%)	Solidus (°C)	Liquidus (°C)
U–19.3 Zr	1216±7	1358±10
	1204(calc.)	1354(calc.)
U–19.5 Pu–3.3 Zr	996±5	1050±4
	974(calc.)	1049(calc.)
U–19.3 Pu–14.5 Zr	1093±8	1321±23
	1022(calc.)	1194(calc.)

A comparison of measured and calculated values for the alloys listed in Table 1 is quite instructive even though only three compositions have been studied to date. For the first alloy, a U–Zr binary, the calculated values agree very well with those measured. Although only one composition has been examined, this agreement, to some extent, lends support to the thermodynamic assessment of that system given above. In particular, much poorer agreement would have resulted had we chosen the heat of fusion of uranium recommended by Oetting et al. (6). The uncertainty estimates, based solely on our thermodynamic evaluation, may be too large. For the second alloy listed in Table 1, a ternary with low Zr content, we find excellent agreement between measured and calculated values for the liquidus and somewhat poorer agreement for the solidus. Because of the low concentration of Zr in this alloy, comparison can be made with uncertainty estimates for the U–Pu system. Our uncertainty estimates for the U–Pu system reflected the fact that the liquidus was much better established than the solidus. These measurements support that conclusion. For the third alloy listed in Table 1, we find poor agreement with the calculations for both the liquidus and the solidus. In contrast to the good agreement found for alloys near the binary edges of the ternary diagram, poor agreement was found for this alloy closer to the center.

It may be that ternary interactions are occurring which are poorly represented by eq. 10. Examination of additional alloy compositions is needed.

4. Conclusions

Calculations have been performed of solidus and liquidus temperatures for the U–Pu–Zr system. Assessment of the three binary sub–systems has revealed an inconsistency with the recommended (6) enthalpy of fusion of uranium. Measurements were performed of solidus and liquidus temperatures for three alloys. The calculated results agree reasonably well with measured values for the two alloys with compositions close to binary edges of the ternary diagram. For the third alloy with a composition further into the ternary diagram, poor agreement was found. Modifications of the calculation for ternary excess Gibbs energies may be required to obtain better agreement between observed and calculated data. Additional alloy compositions are under study.

References

1. J.H. Kittel, J.E. Ayer, W.N. Beck, M.B. Brodsky, D.R. O'Boyle, S.T. Zegler, F.H. Ellinger, W.N. Miner, F.W. Schonfeld, and R.D. Nelson, Nucl. Eng. 15, 373 (1971).
2. C.W. Bale, A.D. Pelton, and W.T. Thompson, "F*A*C*T Users' Instruction Manual," McGill University/Ecole Polytechnique, Montreal (1979-84).
3. P.J. Spencer and I. Barin, Mater. Eng. Appl. 1, 167 (1979).
4. I. Ansara, Internat. Met. Rev., Review 238 , no. 1, 20 (1979).
5. A.D. Pelton, Ch. 7 in "Physical Metallurgy," 3rd edition, eds. R.W. Cahn and P. Haasen, North-Holland, N.Y. (1984).
6. F.L. Oetting, M.H. Rand, and R.J. Ackermann, "The Chemical Thermodynamics of Actinide Elements and Compounds - Part I," Int'l Atom. En. Agency, Vienna (1976).
7. JANAF Thermochemical Tables, Nat'l Bureau of Standards, Washington (1971).
8. H.P. Stephens, High Temp. Sci. 6, 156 (1974).
9. L.S. Levinson, J. Chem. Phys. 40, 3584 (1964).

10. H. Savage and R.D. Seidel, Argonne National Laboratory Report ANL-6702, (1963).

11. K.K. Kelley, U.S. Bur. Mines Bull., 584 (1960).

12. M.H. Rand and O. Kubaschewski, "The Thermochemical Properties of Uranium Compounds", Oliver and Boyd, London (1963).

13. J.A.C. Marples, J. Less-Common Met. 2, 331 (1960).

14. A.A. Bochvar et al., Proc. U. N. Intern. Conf. on Peaceful Uses of Atomic Energy, Geneva, Vol. 6, pp. 184-93 (1958).

15. M. Hansen, "Constitution of Binary Alloys," McGraw-Hill, N.Y. (1958).

16. R.P. Elliott, "Constitution of Binary Alloys - First Supplement," McGraw-Hill, N.Y. (1965).

17. F.A. Shunk, "Constitution of Binary Alloys - Second Supplement," McGraw-Hill, N.Y. (1969).

18. J.M. Taylor, J. Nucl. Mat. 30, 346 (1969).

19. Mound Laboratory Report MLM-1346 (1967).

20. F.H. Ellinger, R.O. Elliott, and E.M. Cramer, J. Nucl. Mat. 3, 233 (1959).

21. Mound Laboratory Report, MLM-1402 (1967).

22. S. Rosen, M.V. Nevitt, and J.J. Barker, J. Nucl. Mat. 9, 128 (1963).

23. P. Chiotti, V.V. Akhachinskij, I. Ansara and M.H. Rand, "The Chemical Thermodynamics of Actinide Elements and Compounds - Part 5," Int'l. At. En. Agency, Vienna (1981).

24. A.D. Pelton, Ber. Bunsenges, Phys. Chem. 84, 212 (1980).

25. D. Summers-Smith, J. Inst. Metals 83, 277 (1954-1955).

26. S.T. Zegler, Argonne National Laboratory Report ANL-6055 (1962).

27. F. Kohler, Monatsch. Chemie 91, 738 (1960).

List of Figures

Fig. 1: Pu-Zr phase diagram

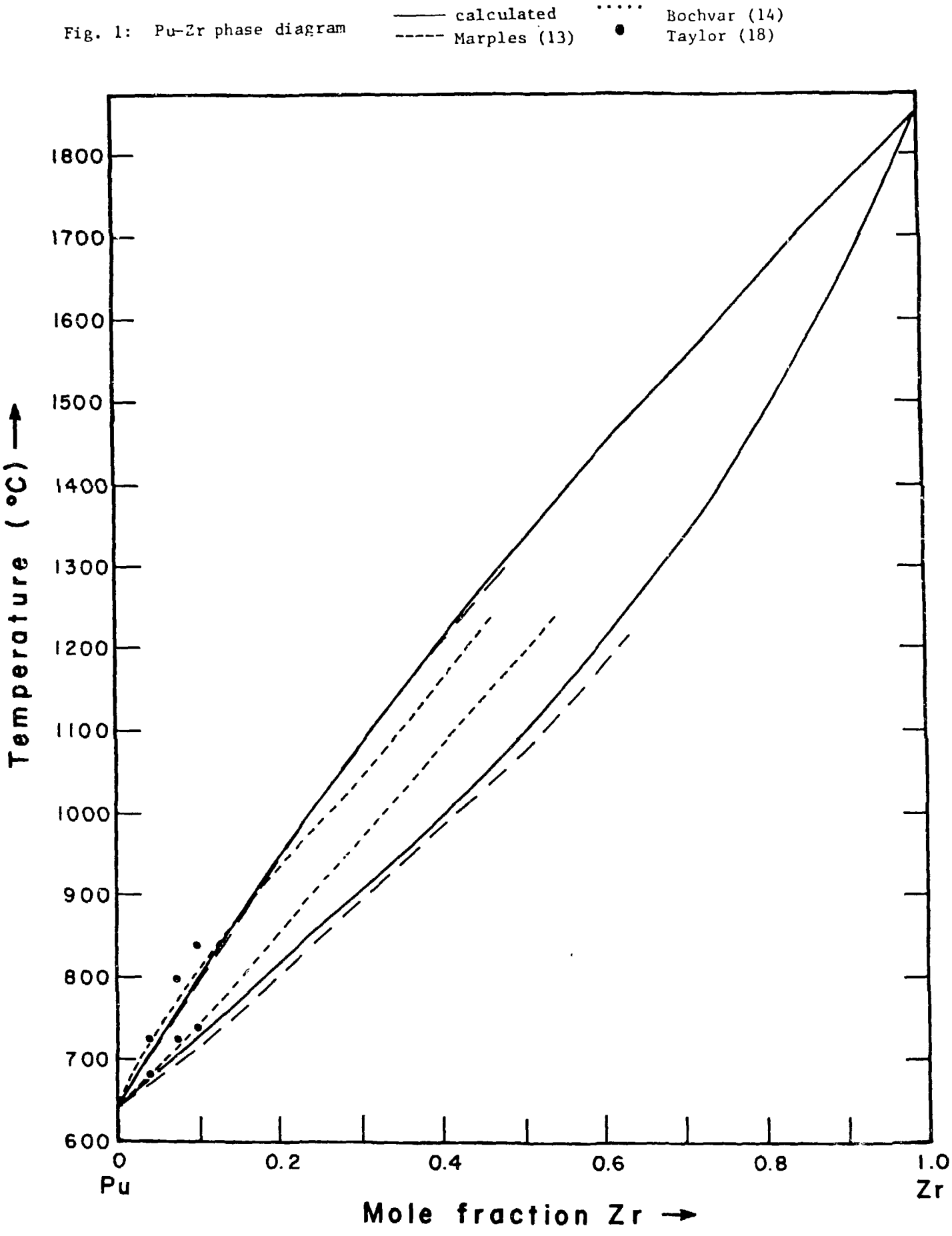

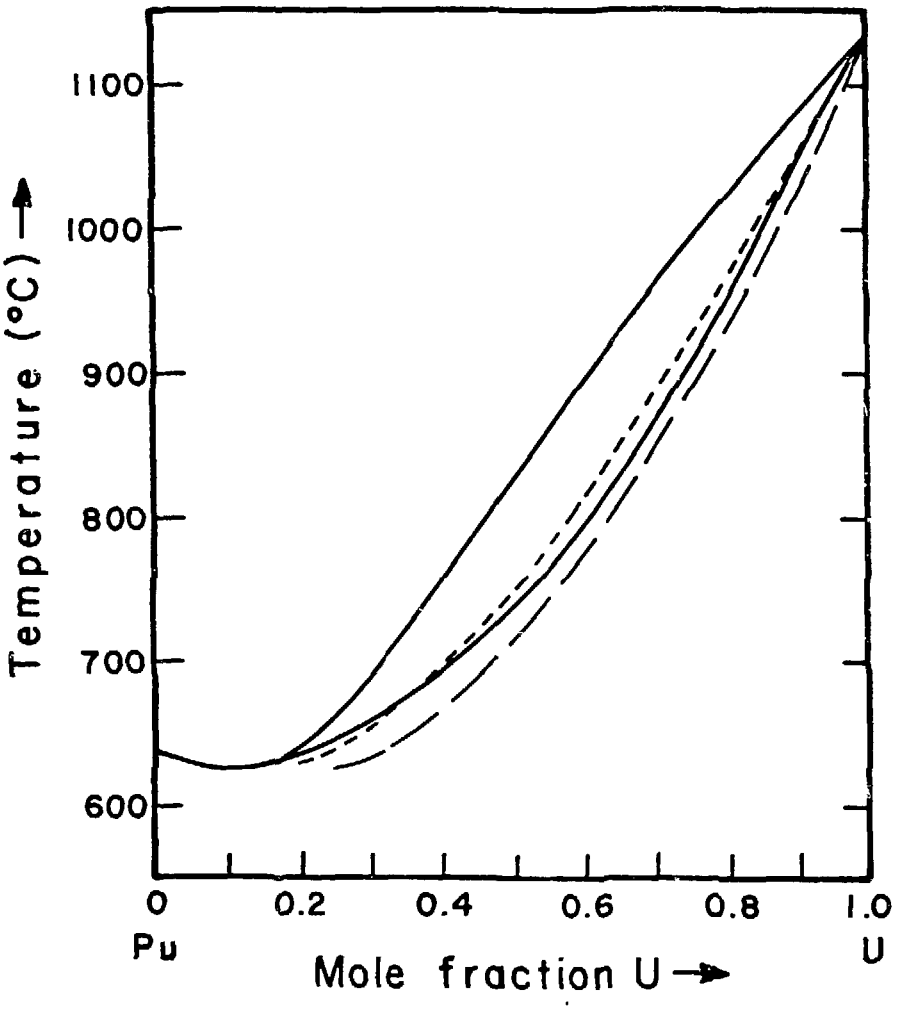

Fig. 2: Pu-U phase diagram

———— Calculated
--------- Ellinger (20)
..... Mound (21)

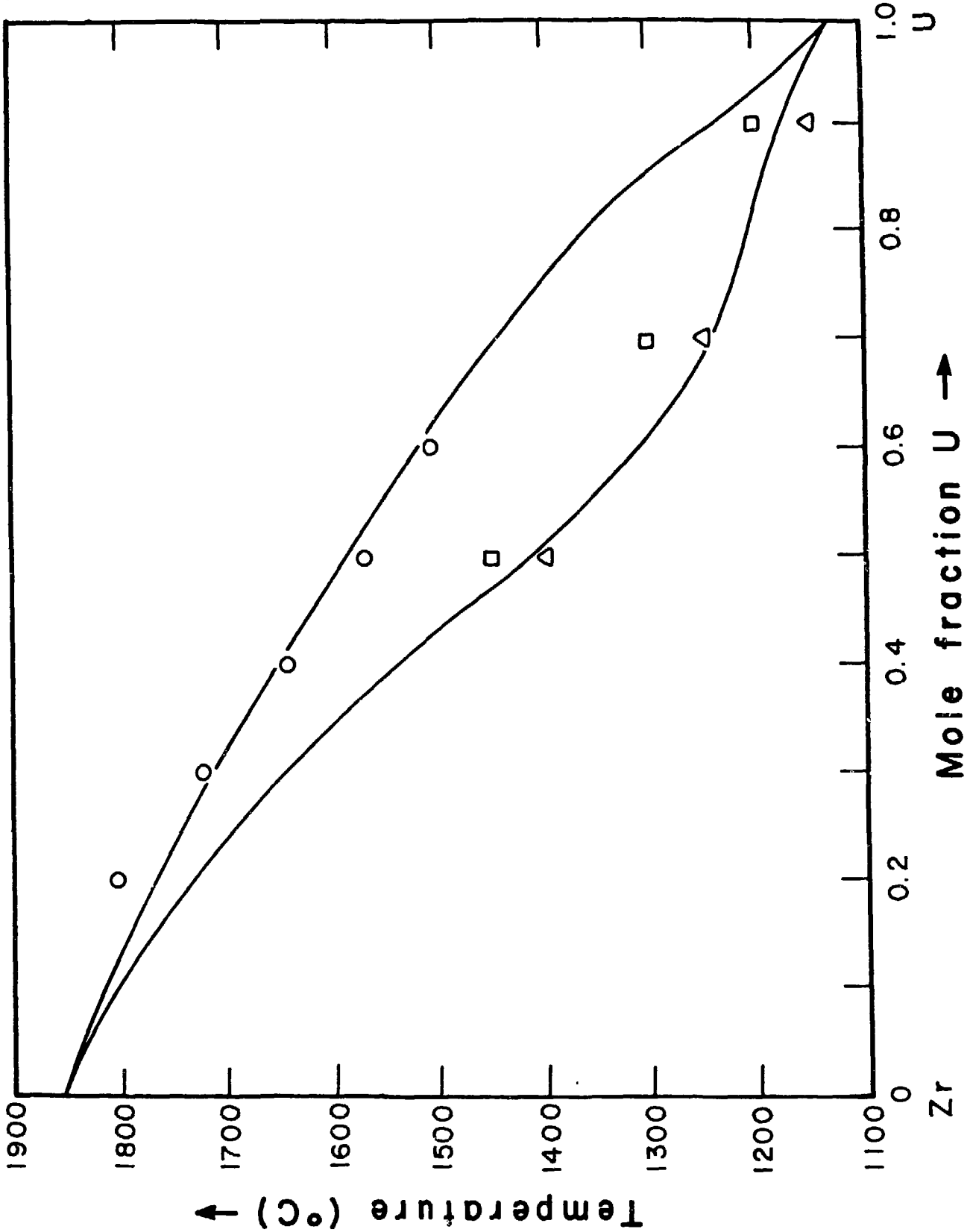

Fig. 3: Zr-U phase diagram

——— Calculated
Points from Summers-Smith (25)

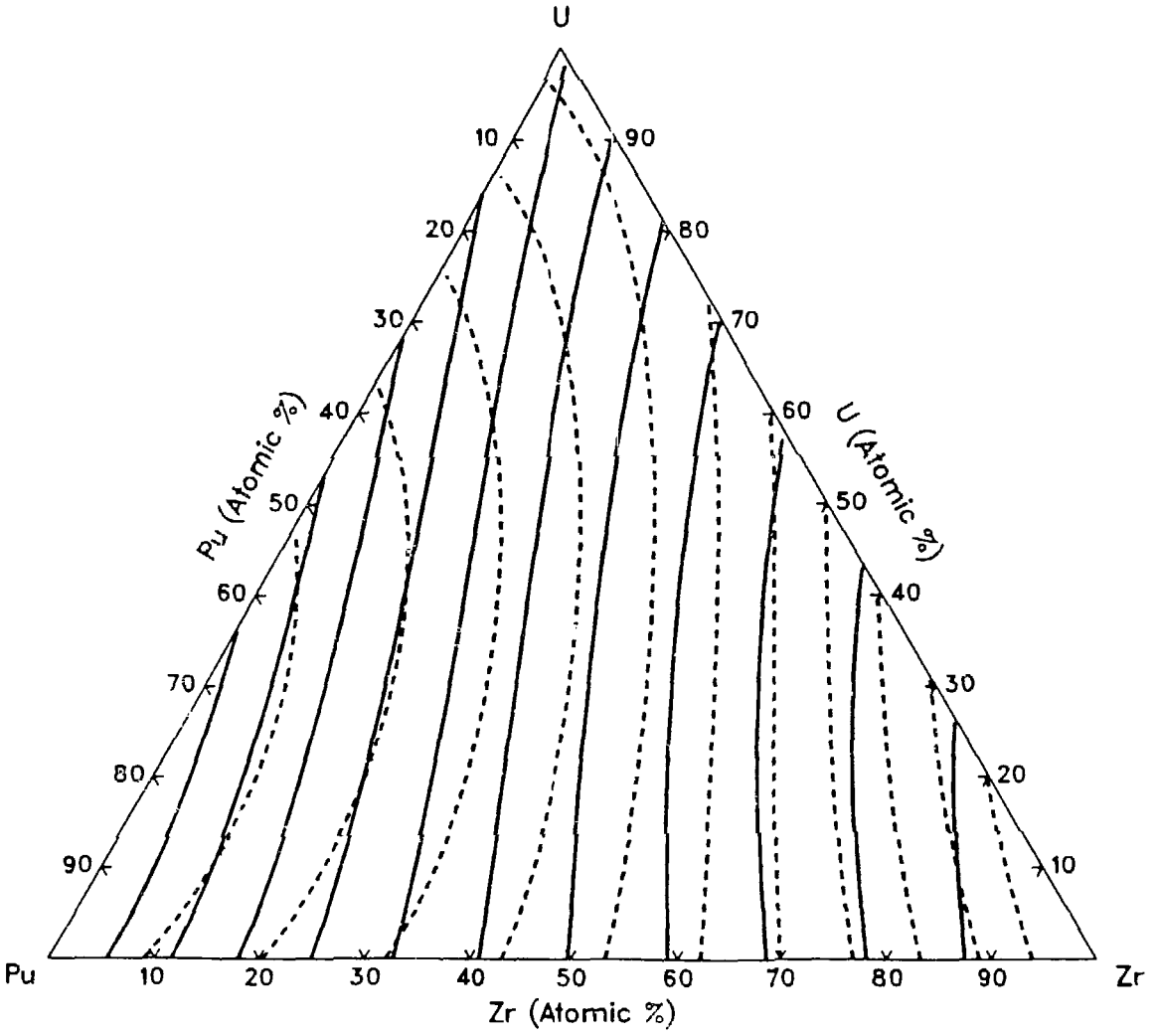

Fig. 4. Calculated polythermal projection of liquidus (solid lines) and solidus (dashed lines) for the U-Pu-Zr system. Temperatures range from 1000 K at the Pu corner to 2000 K at the Zr corner (inclusive) in 100 K intervals.

Fig. 5. As-cast U-19.3 at.% Pu - 14.5 at.% Zr showing globular Zr inclusions.

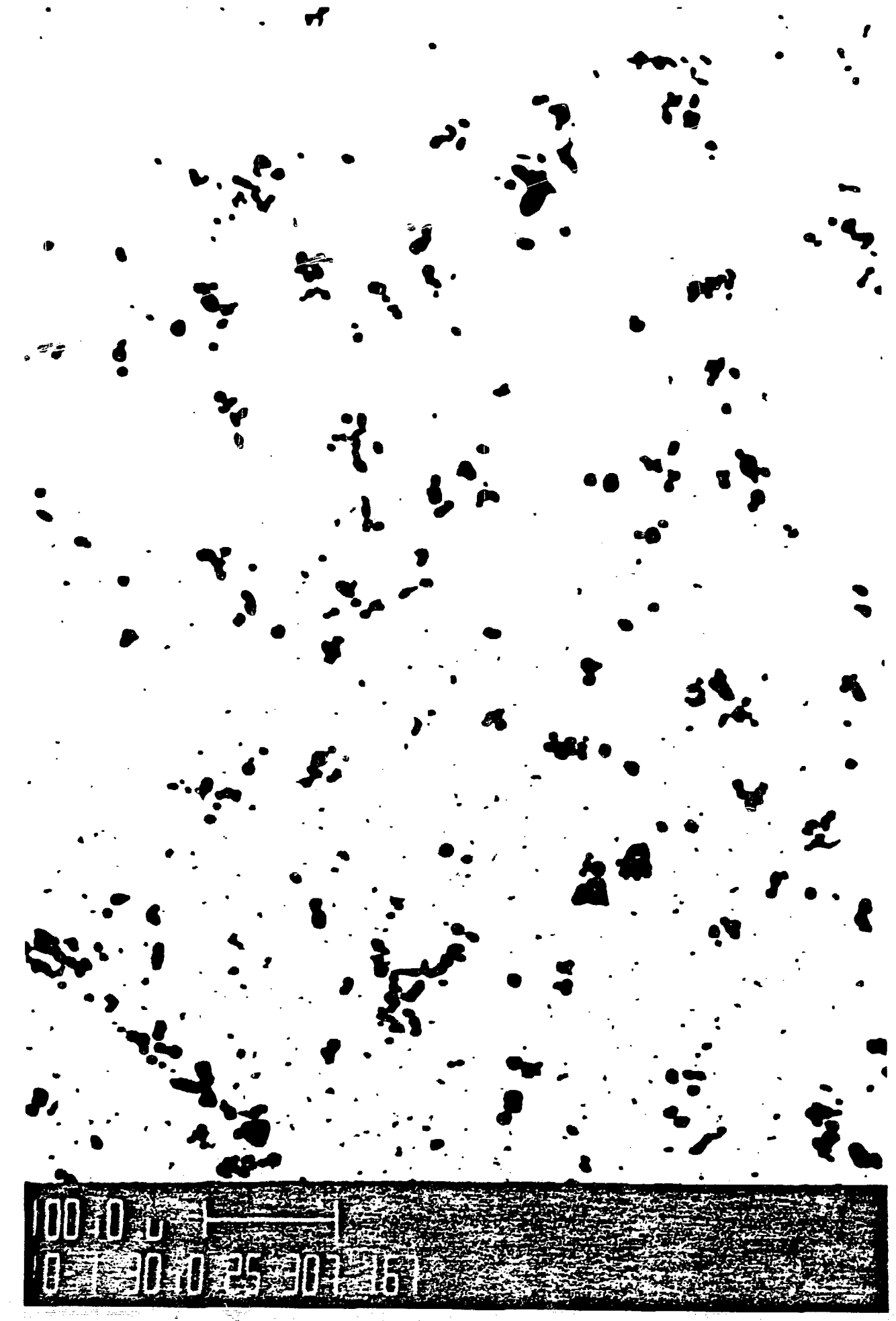

Fig. 6. Thick Zr-rich layer on top of sample following melting.

00 10 u
5 1 30 0 23 006 073

Fig. 7. Small U-Pu-rich inclusions (bright areas) in (dark) Zr-rich globular phase.